

Chemical Science



Accepted Manuscript

This article can be cited before page numbers have been issued, to do this please use: X. Zhao, X. Chen, L. Fan, Y. Jiang, Y. Chen, D. Song, F. Ling, J. Hu and W. Zhong, *Chem. Sci.*, 2025, DOI: 10.1039/D5SC08462H.



This is an Accepted Manuscript, which has been through the Royal Society of Chemistry peer review process and has been accepted for publication.

Accepted Manuscripts are published online shortly after acceptance, before technical editing, formatting and proof reading. Using this free service, authors can make their results available to the community, in citable form, before we publish the edited article. We will replace this Accepted Manuscript with the edited and formatted Advance Article as soon as it is available.

You can find more information about Accepted Manuscripts in the <u>Information for Authors</u>.

Please note that technical editing may introduce minor changes to the text and/or graphics, which may alter content. The journal's standard <u>Terms & Conditions</u> and the <u>Ethical guidelines</u> still apply. In no event shall the Royal Society of Chemistry be held responsible for any errors or omissions in this Accepted Manuscript or any consequences arising from the use of any information it contains.



View Article Online DOI: 10.1039/D5SC08462H

ARTICLE

Received 00th January 20xx. Accepted 00th January 20xx

DOI: 10.1039/x0xx00000x

Bulky alkali metal cations enabled highly efficient iridiumcatalyzed asymmetric hydrogenation for C-N axial chirality via dynamic kinetic resolution

Xianghua Zhaoa, Xinyu Chena, Linxian Fana, Yulong Jianga, Yirui Chena, Dingguo Songc, Fei Linga*, Junyuan Hub* and Weihui Zhonga*

The addition of excess alkali metal to Noyori-type catalysts (HM-NH) generates anionic species (HM-NM'), which significantly enhances both the reaction rate and turnover number (TON) in asymmetric hydrogenation. However, such anionic catalysts have been largely confined to the construction of central chirality, with few reports on application to axial chirality. Herein, we report a highly efficient anionic iridium catalyst (HIr-NCs) based on a newly tridentate ligand framework (Huaphos), which enables the asymmetric hydrogenation of N-aryl indole ketones (and aldehydes) via dynamic kinetic resolution under mild conditions, allowing for the construction of axial chirality with excellent stereocontrol (up to >99% ee and >99:1 dr). DFT studies indicate that strong electrostatic interaction between the bulky cesium cation and the oxygen atom of the substrate dramatically reduces the activation barrier, resulting in a substantially accelerated reaction rate for the anionic Ir catalyst (Hir-NCs) compared to the neutral Ir/Huaphos system (Hir-NH). In the presence of anionic Ir catalyst, this protocol can be scaled up to gram quantities under an exceptionally low catalyst loading (S/C = 40,000), and the resulting hydrogenation product can be further transformed into novel chiral ligands that show promise in asymmetric catalysis.

Introduction

The asymmetric hydrogenation of carbonyl compounds stands as a pivotal methodology in fine chemical and pharmaceutical synthesis. Early catalytic systems predominantly followed inner-sphere mechanisms, showing modest efficiency.[1] This model shifted with the introduction of Noyori-type HM-NH bifunctional catalysts, which revolutionized the field through their outer-sphere mechanism, achieving unprecedented levels of enantiocontrol and catalytic turnover.^[2] Mechanistic studies have established that these catalysts engage the substrate through cooperative metal-hydride (M-H) and N-H functionalities, enabling a concerted hydrogen transfer via hydrogen bonding (Scheme 1A).[3] Since then, asymmetric hydrogenation catalysts developed by numerous scientists worldwide, such as Zhou, [4] Zhang, [5] Morris, [6] Clarke, [7] Beller [8] and others^[9]. have largely followed this model.

With the continuous advancement of asymmetric hydrogenation, the design of more efficient catalysts has become crucial for

achieving higher activity and efficiency. Compared to neutral catalysts, anionic metal complexes-bearing formal negative chargescan increase the electronegativity of metal-bound hydride atoms, [10] potentially enhancing catalytic performance. The use of anionic catalysts in homogeneous hydrogenation dates back to the 1980s, when Pez and colleagues demonstrated their unique advantages.[11] Since then, the concept of anionic catalysis has been successfully applied to other catalytic transformations.[12] These developments have inspired efforts to incorporate anionic motifs into the established MH-NH system, to exploit their inherent reactivity advantages. In 2001, it was reported that the addition of excess base plays a crucial role in maintaining the high activity of Noyori-type catalysts, [13] leading to the proposal of a more efficient HM-NM' model in which a deprotonated amino group (N-M') operates in concert with a metal hydride (M-H).[14] Density functional theory (DFT) calculations support this mechanism, illustrating a stepwise hydrogen transfer process wherein the rate-determining transition state is stabilized by noncovalent interactions (Scheme 1A).[14] Further evidence for the involvement of such anionic species comes from the structural and spectroscopic characterization of alkali metal-hydride-amidate complexes, demonstrating their existence and potential role as active intermediates. [15] Beyond the extensively studied HM-NM' class of catalysts, Poli et al. reported on iridium systems that, although not deprotonated, still exhibit behavior consistent with anionic catalysis, likely because strong bases generate transient anionic species. Their work underscores the broader relevance of anionic pathways and the critical role of strong bases in enabling high catalytic efficiency. [16] Additional implementations of the MH-NM' system have since been

^aState Key Laboratory of Green Chemical Synthesis and Conversion, College of Pharmaceutical Sciences, Zhejiana University of Technology, Hangzhou 310014, P. R.

E-mail: lingfei@zjut.edu.cn; weihuizhong@zjut.edu.cn

bSchool of Chemistry and Chemical Engineering, Shandong University, Jinan, 250100, People's Republic of China

E-mail: hujy2023@163.com

^cHuzhou Key Laboratory of Medical and Environmental Applications Technologies, School of Life Sciences, Huzhou University, Huzhou 313000, P. R. China

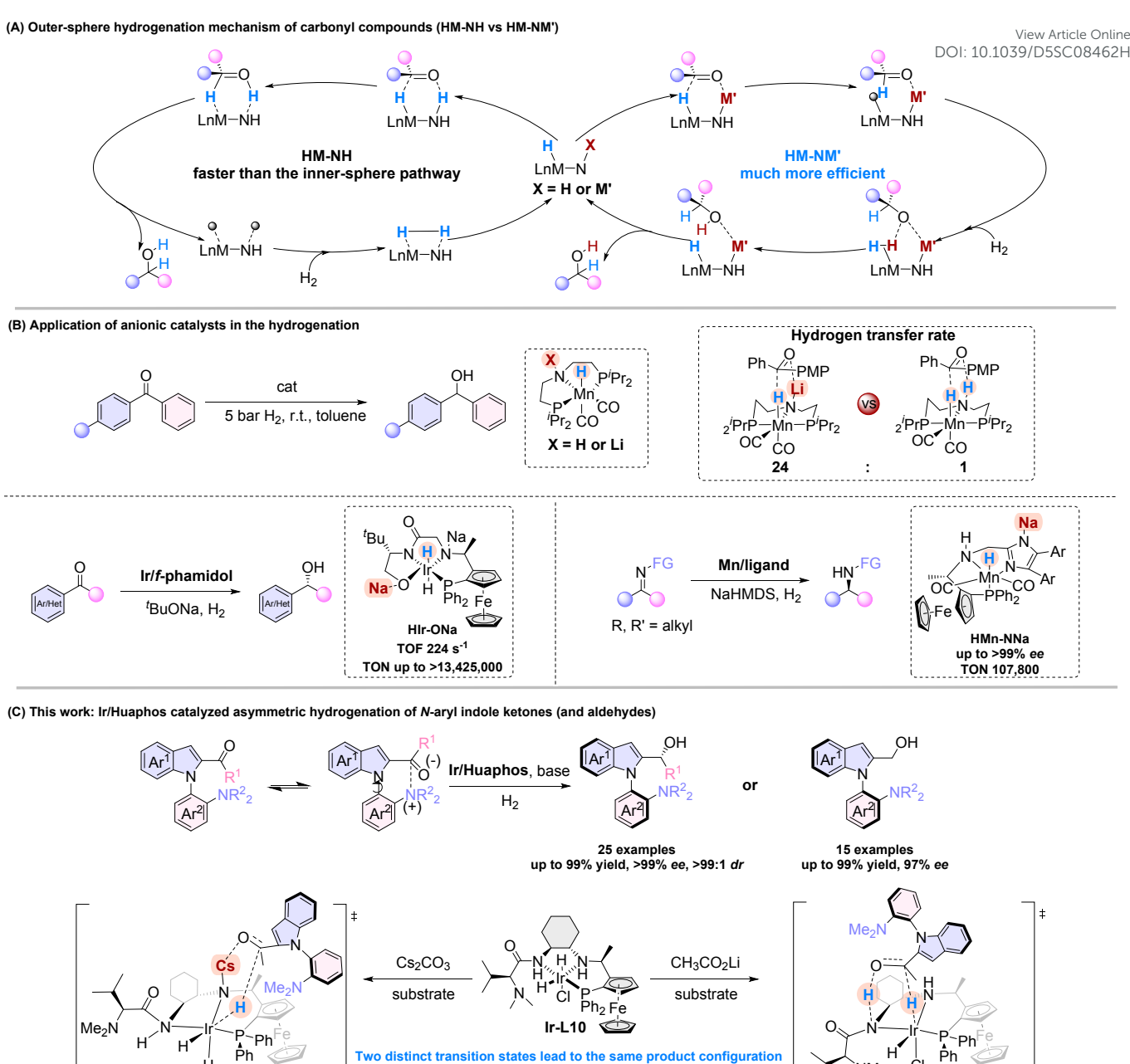
[†]Supplementary Information available: [details of any supplementary information available should be included here]. See DOI: 10.1039/x0xx00000x

Journal Name

ARTICLE

This article is licensed under a Creative Commons Attribution-NonCommercial 3.0 Unported Licence

Open Access Article. Published on 27 November 2025. Downloaded on 28.11.2025 06:55:37



Scheme 1. (A) Outer-sphere hydrogenation mechanism of carbonyl compounds; (B) Previous reports; (C) This work.

Broad substrate scope and good functional group tolerance

Low catalyst loading

Detailed machanistic studies

documented, underscoring its general utility in catalytic hydrogenation. [17]

HIr-NCs bifunctional pathway ($\Delta G = -4.6 \text{ kcal/mol}$)

In 2022, Liu^[17a] first synthesized and characterized a lithium manganese hydride amidate complex (HMn-NLi). Kinetic studies and DFT calculations revealed that HMn-NLi reacts with ketones 24-fold faster than its parent amino hydride (HMn-NH), due to the significantly stronger affinity between the N-Li moiety and carbonyl groups compared to the N-H group, demonstrating the superiority of metal-assisted hydrogen transfer (**Scheme 1B**). In 2023, Zhang^[17b] combined the concept of anionic catalysts with multidentate ligands

to develop a class of tetradentate anionic iridium catalysts exhibiting exceptional efficiency in the asymmetric hydrogenation of ketones (TOF = 224 s⁻¹, TON up to 13,425,000, **Scheme 1B**). Liu and colleagues^[17c] extended anionic catalysis to chiral manganese systems, enabling the asymmetric hydrogenation of dialkyl ketimines (**Scheme 1B**). Comprehensive structural and mechanistic studies confirmed that both catalyst architecture and cation participation enhance enantioselectivity. These examples highlight the superior performance of catalysts based on the HM-NM' model. However, its application has so far been largely restricted to systems involving

Excellent diastereo- and enantioselectivities

Synthetic applications with potenial value

HIr-NH cooperative mechanism ($\Delta G = 26.0 \text{ kcal/mol}$)

This article is licensed under a Creative Commons Attribution-NonCommercial 3.0 Unported Licence

pen Access Article. Published on 27 November 2025. Downloaded on 28.11.2025 06:55:37

ARTICLE Journal Name

Table 1. Optimization of reaction conditions

 $L7:R^1 = Bn, R^2 = Boc, R^3 = H$ **L8**: $R^1 = {}^{i}Pr$, $R^2 = Boc$, $R^3 = CH_2$

L9: $R^1 = {}^tBu$, $R^2 = Boc$. $R^3 = CH$.

L10: $R^1 = {}^{i}Pr$, $R^2 = CH_3$, $R^3 = CH_3$

					<u> </u>	<u>ت</u>
Entry	Ligands	Bases	Solvents	Conv. (%)	ee (%)	dr
1	L1	[‡] BuOLi	[/] PrOH	10	20	1:1
2	L2	^t BuOLi	[/] PrOH	15	28	1:1
3	L3	^t BuOLi	[/] PrOH	50	52	4:1
4	L4	^t BuOLi	[/] PrOH	60	58	17:3
5	L5	^t BuOLi	[/] PrOH	55	56	4:1
6	L6	^t BuOLi	[/] PrOH	58	53	4:1
7	L7	^t BuOLi	[/] PrOH	57	50	5:1
8	L8	^t BuOLi	[/] PrOH	55	58	9:1
9	L9	^t BuOLi	[/] PrOH	50	56	9:1
10	L10	^t BuOLi	[/] PrOH	70	65	20:1
11	L10	^t BuOLi	EA	80	78	20:1
12	L10	^t BuOLi	THF	78	76	9:1
13	L10	^t BuOLi	toluene	86	82	20:1
14 ^b	L10	CH₃CO₂Li	toluene	99	>99	>99:1
15	L10	Cs ₂ CO ₃	toluene	99	>99	>99:1
16 ^c	L10	Cs ₂ CO ₃	toluene	15	85	20:1

^aReaction conditions: **1a** (0.25 mmol), [Ir(COD)CI]₂ (0.05 mol%), ligand (0.11 mol%), base (10 mol%), solvent (1 mL), 50 °C, H_2 (5 MPa) and 12 h. The conversion was determined by GC analysis. The ee and dr values were determined by HPLC analysis. b36 h. c21-crown-7 (0.25 mmol) was used as the additive

small alkali metal cations, and in asymmetric hydrogenation, it remains primarily limited to the construction of central chirality, with very few reports on the synthesis of axially chiral compounds.

Axial chirality represents an important class of molecular frameworks that are widely present in natural products, pharmaceuticals, functional materials, bioactive molecules, as well as privileged chiral ligands and organocatalysts.[18] As a result, significant efforts have been made over the past two decades to develop efficient strategies for constructing axial chirality.[19] However, to date, only a few examples^[20] have employed asymmetric hydrogenation for the construction 1049 ax fails of the construction asymmetric hydrogenation for the construction of the construction compounds. Despite these reports, challenges remain, including limited substrate scope, suboptimal stereoselectivity, high catalyst loading, and poorly defined catalyst properties.

In response to these challenges, we herein report a novel class of chiral ligands (Huaphos) building on our previous work in ligand design,[21] which were successfully used in iridium-catalyzed asymmetric hydrogenation of configurationally labile N-aryl indole ketones (and aldehydes), affording excellent stereoselectivities (up to >99% ee, >99:1 dr). Spectroscopic analysis revealed that the neutral Ir/Huaphos complex (HIr-NH) is activated by cesium carbonate to generate a novel anionic iridium catalyst (HIr-NCs). DFT calculations further indicate that the large cesium cation engages in a significant electrostatic interaction with the oxygen atom of the substrate, which substantially lowers the activation barrier and accelerates the reaction rate. This cation-substrate interaction, enabled by the bulky Cs+, represents a key design element for achieving high efficiency. With the aid of anionic iridium catalyst (HIr-NCs), this protocol can be scaled up to gram quantities using a low catalyst loading (S/C = 40,000). The resulting hydrogenation products can be further transformed into novel chiral ligands, which show promising applications in asymmetric catalysis.

Results and discussion

Reaction Optimization. The chiral Huaphos ligands can be readily synthesized using well-established methods in 50-75% yields (Supporting Information, Page S1). With the ligands in hand, we proceeded to investigate their application in the asymmetric hydrogenation of N-aryl indole ketones.

In the initial study, 1-(1-(2-(dimethylamino)phenyl)-1H-indol-2-yl) ethan-1-one (1a) was chosen as the model substrate, with 'BuOLi as the base and 'PrOH as the solvent to evaluate a series of catalytic systems. We first tested the efficacy of Ir/f-diaphos that had demonstrated exceptional results in the asymmetric hydrogenation of simple ketones. Disappointedly, it delivered only low yield and poor stereoselectivity (entries 1-2). Subsequently, the new catalytic system was evaluated under identical conditions, affording the desired product in moderate yield and stereoselectivity. To explore the substituent effects on catalytic performance, a series of amino acid-derived ligands were systematically assessed. Among them, L10 proved optimal, providing the highest yield and stereoselectivity (entries 3-10). Following a systematic screening of solvents and bases, Cs₂CO₃ and toluene were identified as the optimal system, providing the highest stereoselectivity (>99% ee, >99:1 dr) and fastest reaction rate (complete in 12 h). Although CH₃CO₂Li delivered comparable stereoselectivity (with CH₃CO₂Na and CH₃CO₂Cs showing slightly lower selectivity), the transformation required 36 hours to reach full conversion (entries 11-15 and Supporting Information, Page S18-19, Table S1 and S2). Moreover, the inclusion of one equivalent of 21-crown-7 as a cesium cation sequestering agent led to a significant decrease in conversion. The above results suggest that CH₃CO₂Li (a weak base) and Cs₂CO₃ (a strong base) may play distinct roles in the reaction. As a result, the optimal reaction conditions were identified as follows: [Ir(COD)Cl]₂/L10 (0.1 mol%) as

Scheme 2. Substrate scope of N-aryl indole ketones

This article is licensed under a Creative Commons Attribution-NonCommercial 3.0 Unported Licence

Open Access Article. Published on 27 November 2025. Downloaded on 28.11.2025 06:55:37

View Article Online DOI: 10.1039/D5SC08462H

^aReaction conditions: 1 (0.25 mmol), [Ir(COD)Cl]₂ (0.05 mol%), L10 (0.11 mol%), Cs₂CO₃ (10 mol%), toluene (1 mL), 50 °C and H₂ (5 MPa). Isolated yields were obtained by flash chromatography and the ee and dr values were determined by HPLC analysis. bCH₃CO₂Li was used as the base instead of Cs₂CO₃.

catalyst, Cs₂CO₃ (10 mol%) as base, toluene as solvent, under 5 MPa H₂ at 50 °C.

Substrate Scope. With the optimized conditions established, the substrate scope of the iridium-catalyzed dynamic kinetic resolution (DKR) of ketones for the construction of C-N axial chirality was explored (Scheme 2). To elucidate the distinct roles of Cs₂CO₃ and CH₃CO₂Li in the reaction, both bases were evaluated under otherwise identical conditions. We initially investigated a series of N-aryl indole ketones bearing substituents at various positions on the indole and benzene rings. Nearly all substrates delivered the corresponding products (2a-2o) with excellent enantioselectivity (>99% ee) and diastereoselectivity (>99:1 dr). Notably, substrates bearing electronwithdrawing groups (1d, 1f-1h, 1k) exhibited significantly faster reaction rates compared to those with electron-donating groups (1b, 1c, 1e, 1i, 1j, 1l-1o), suggesting a beneficial electronic effect on the reaction kinetics. The absolute configuration of this class of products was unambiguously determined for the first time through X-ray crystallographic analysis of compound 2g. Comparative studies revealed that reactions employing Cs2CO3 as base proceeded significantly faster than those with CH₃CO₂Li, while maintaining comparable stereoselectivity. Notably, when Cs₂CO₃ was employed as the base, the 3-methyl-substituted substrate 1b was efficiently converted to 2b, whereas CH₃CO₂Li afforded only low yield under identical conditions. Next, we evaluated aliphatic acyl and diaryl

This article is licensed under a Creative Commons Attribution-NonCommercial 3.0 Unported Licence.

Open Access Article. Published on 27 November 2025. Downloaded on 28.11.2025 06:55:37

Journal Name

substrates (1p-1w) under the standard conditions. Similar to the results observed with 1b, these substrates showed low conversion rates when CH₃CO₂Li was used as the base. After replacing the base with Cs₂CO₃, complete conversion was achieved for substrates 1p-1w. The corresponding hydrogenation products were obtained with high stereoselectivity: **2p** (>99% ee, >99:1 dr), **2q** (95% ee, 49:1 dr), and 2s (92% ee, 47:3 dr). Interestingly, during the hydrogenation of substrates containing a vinyl substituent (Supporting Information, Page S15, substrate 1y), the terminal C=C bond was also completely reduced, leading to the formation of the desired product 2p' in similar yield and stereoselectivity. This unexpected observation reveals the robustness of the catalytic system and suggests new opportunities for the Huaphos ligand in broader catalytic transformations. However, the cyclopropyl-substituted product (2r) showed reduced stereoselectivity (60% ee, 93:7 dr), likely due to the inherent rigidity of the three-membered ring system. Substrate bearing an *n*-hexyl group was also successfully transformed into the corresponding product (2t) with up to >99% ee, >99:1 dr. Replacing the alkyl group with a phenyl group (2u), led to a sharp drop in enantioselectivity to 10% ee (3:1 dr), presumably due to restricted rotation and increased steric congestion from the aromatic ring. To address this limitation, we introduced a two-carbon spacer between the phenyl ring and the carbonyl group prior to hydrogenation. As expected, this structural modification restored both high yield and excellent stereoselectivity in the resulting product (2v). Finally, substrates derived from cyclopentylamine and cyclohexylamine were also compatible, delivering **2w** (>99% *ee*, >99:1 *dr*) and **2x** (98% ee, 99:1 dr), respectively, regardless of the base used. These results collectively demonstrate the broad applicability and versatility of the Ir/Huaphos catalytic system in constructing C-N axially chiral architectures.

Synthetic Application. To demonstrate the practicality of the developed strategy, a gram-scale hydrogenation of 1a (2.78 g) was

performed under 5 MPa of H₂ at 50 °C, using a low catalyst loading (S/C = 40,000) for 30 hours to afford the corresponding product 2a with up to >99% ee and >99:1 dr (Scheme 3A). The hydroxyl group in 2a was then converted into an amino group with inversion of configuration via a classic Mitsunobu reaction^[22] yielding chiral amine 3a (Scheme 3B). Chiral amines serve as valuable synthetic building blocks, enabling the efficient synthesis of a wide range of chiral ligand architectures. [23] For example, 3a was condensed with 3,5-bis(trifluoromethyl)phenyl isothiocyanate to afford a novel bifunctional thiourea catalyst 4a in 90% yield and 95% ee (Scheme **3C**). In addition, chiral amine **3a** could be further transformed into chiral P/N ligands 5a and 6a through amide condensation and reductive amination respectively (Scheme 3D-3E). The chiral P/N ligand frameworks exhibit remarkable versatility in asymmetric transformations. [24] Notably, the bidentate ligand 6a was successfully applied in the asymmetric hydrogenation of acetophenone, affording the secondary alcohol product **7a** with 77% ee (**Scheme 3F**). This application underscores the synthetic value and promising potential of the ligand architecture derived from this catalytic DKR strategy. Furthermore, we conducted a preliminary investigation into the catalytic performance of 4a in asymmetric transformations (Supporting Information, Page S36).

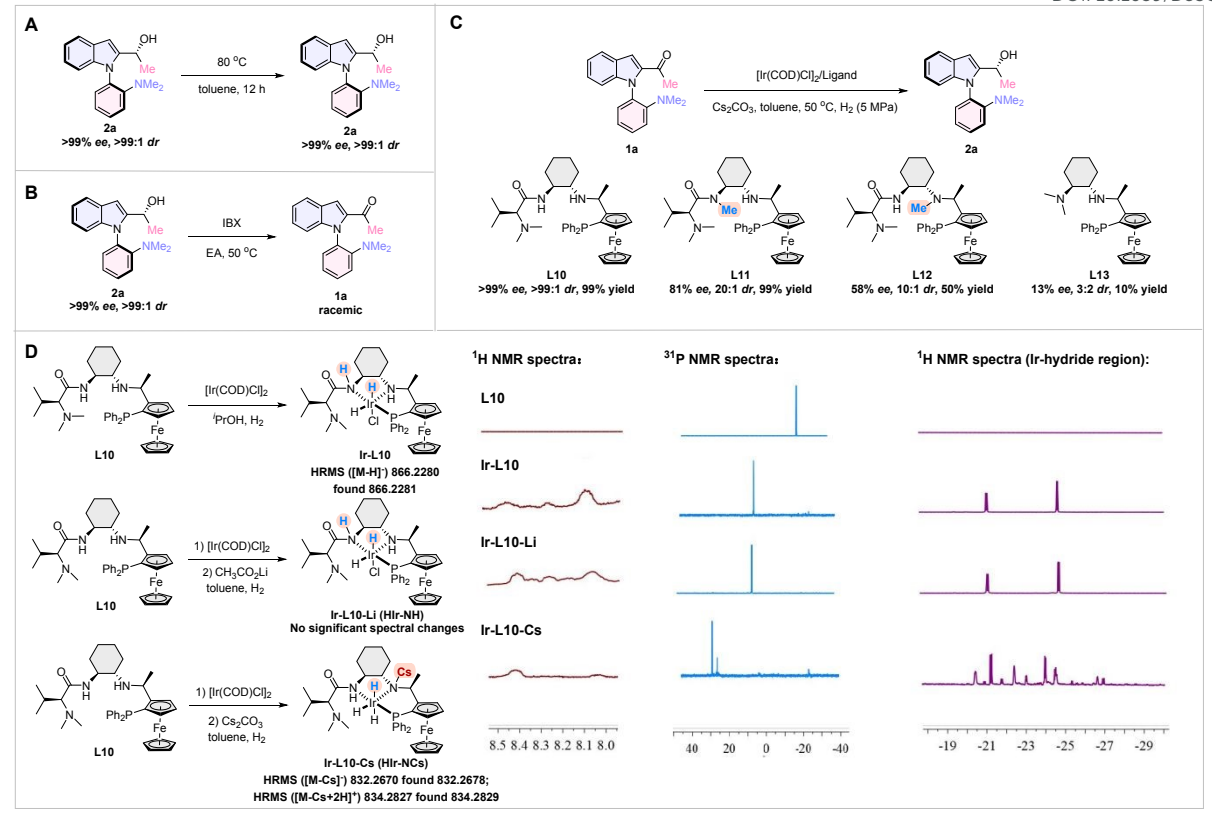
Mechanistic Studies. As reported in the literature, [19j] a weak Lewis acid-base interaction exists between the carbonyl group of the analogous aldehyde substrate and the adjacent NMe2 moiety, facilitating rotation around the C-N bond through a six-membered cyclic transition state. This conformational lability enables rapid racemization, fulfilling a key requirement for an effective dynamic kinetic resolution (DKR) process-fast substrate racemization under the reaction conditions. This mechanistic rationale is further supported by DFT calculations. To experimentally validate this hypothesis, we first investigated the configurational stability of the C-N axial chirality through racemization studies. When compound 2a

Scheme 3. Gram scale synthesis of 2a and its transformations

ence Accepted Manuscrip

Scheme 4. Control experiment and spectroscopic characterization of the catalyst

View Article Online DOI: 10.1039/D5SC08462H



was stirred in toluene at 80 °C for 12 hours, chiral HPLC analysis revealed no discernible erosion of enantiomeric excess, indicating high stereochemical stability under these conditions (Scheme 4A, Supporting Information for details, Page S37). Then control experiments were performed. Notably, oxidation of the hydroxyl group in 2a to the corresponding ketone led to complete racemization of the axial chirality (Scheme 4B), consistent with the proposed mechanism. Subsequent DFT calculations of the rotational barriers for 1a and 2a revealed that 1a has a significantly lower barrier (25.8 kcal·mol⁻¹) compared to 2a (36.6 kcal·mol⁻¹). This substantial difference further supports the role of the carbonyl group in reducing rotational energy and facilitating racemization, thus corroborating the proposed DKR mechanism (Supporting Information, page S67).

Informed by previous studies, [15,17] we performed a comprehensive characterization of the catalyst to better understand the nature of the active catalytic species. First, the **Ir-L10** complex was thoroughly characterized using a combination of spectroscopic and analytical techniques. The neutral **Ir-L10** complex was prepared by reacting ligand **L10** with [Ir(COD)Cl]₂ under an H₂ atmosphere. In the 1H NMR spectrum, two new downfield-shifted resonances were observed at δ 8.40 ppm and δ 8.05 ppm (**Scheme 4D**, Supporting Information, Page S42), which were assigned to the amide N-H and amino N-H protons, respectively, upon coordination to the iridium center. This significant deshielding indicates a strong electronic interaction between the nitrogen lone pairs and the metal, consistent with successful formation of the Ir-N bonds. Furthermore, ATR-IR spectroscopy provided compelling evidence for coordination: the N-H stretching vibrations of the amide (from 3454 to 3418 cm $^{-1}$)

and amino groups (from 3381 to 3257 cm⁻¹) shifted to lower wavenumbers, while the carbonyl (C=O) stretch shifted to higher wavenumbers (from 1711 to 1739 cm⁻¹, Supporting Information, Page S41). The ³¹P NMR spectrum showed a significant downfield shift of the phosphorus resonance from δ -25.0 ppm in the free ligand **L10** to δ 7.2 ppm in the **Ir-L10** complex, providing strong evidence for coordination of the phosphine moiety to the iridium center (Scheme 4D, Supporting Information, Page S43). Additionally, two distinct hydride resonances were observed at δ –21.0 ppm and -28.0 ppm in the ¹H NMR spectrum, characteristic of chemically inequivalent Ir-H ligands in an octahedral Ir(III) complex (Scheme 4D, Supporting Information, Page S43). These signals were further corroborated by ATR-IR spectroscopy, which revealed two sharp bands at 2194 cm⁻¹ and 2146 cm⁻¹, consistent with terminal Ir-H stretching vibrations. Together, these data confirm the presence of two hydride ligands bound to the iridium center. Finally, HRMS confirmed the molecular formula of Ir-L10, detecting the [M-H]⁻ ion at m/z 866.2281 (calcd. 866.2280, Supporting Information, Page S39). Taken together with NMR and ATR-IR data, this result unambiguously establishes Ir-L10 as a neutral, tridentate PNN-coordinated iridium(III) complex.

Subsequent mixing of **L10**, [Ir(COD)CI]₂ and CH₃CO₂Li under a hydrogen atmosphere showed no observable changes in its spectroscopic characteristics (**Scheme 4D**, Supporting Information, Page S44-46). In contrast to CH₃CO₂Li, treatment with Cs₂CO₃ induced significant spectroscopic changes in the iridium complex. The ¹H NMR spectrum showed nearly complete disappearance of the resonance at δ 8.05 ppm (assigned to the amino N-H proton), indicating deprotonation of the coordinated amine (**Scheme 4D**,

This article is licensed under a Creative Commons Attribution-NonCommercial 3.0 Unported Licence.

Open Access Article. Published on 27 November 2025. Downloaded on 28.11.2025 06:55:37

Journal Name

Supporting Information, Page S54). Concurrently, the ³¹P NMR signal shifted dramatically from δ 7.2 ppm (in the neutral complex) to δ 31.5 ppm (Scheme 4D, Supporting Information, Page S55), likely reflecting structural reorganization induced by the deprotonation process. ATR-IR analysis further revealed a new Ir-H stretching vibration, suggesting the formation of a third Ir-H ligand (Supporting Information, Page S55), due to chloride dissociation under basic conditions and subsequent hydrogenation under H2. HRMS confirmed the formation of two key species: the [M-Cs]⁻ ion at m/z 832.2678 and the [M-Cs+2H]+ ion at m/z 834.2829 (Supporting Information, Page S53). These data collectively support the formation of an anionic, tridentate coordinated iridium(III) species (Ir-L10-Cs) which serves as a key activated catalyst in the reaction. In addition, we sought to characterize the transformation of the

catalyst under the influence of Cs₂CO₃. Comprehensive spectroscopic analysis by NMR, HRMS, and ATR-IR (Supporting ใค้ชื่อให้เอ็ก คือสู่ย่ S47-55) supports a mechanistic pathway in which the catalyst undergoes simultaneous departure of the amide N-H proton and chloride ligand, deprotonation of the amino N-H group, and oxidative addition of H₂, ultimately forming an anionic active species.

To validate the proposed anionic catalyst model, we synthesized structurally modified versions of ligand L10 and evaluated their performance under standard reaction conditions employing Cs₂CO₃ as base. The amide N-H methylated ligand L11 exhibited modestly reduced enantioselectivity, while the amine N-H methylated ligand L12 showed significantly diminished reactivity and enantioselectivity (Scheme 4C). This stark contrast underscores the critical role of the amine N-H group in catalyst activation, providing strong support for

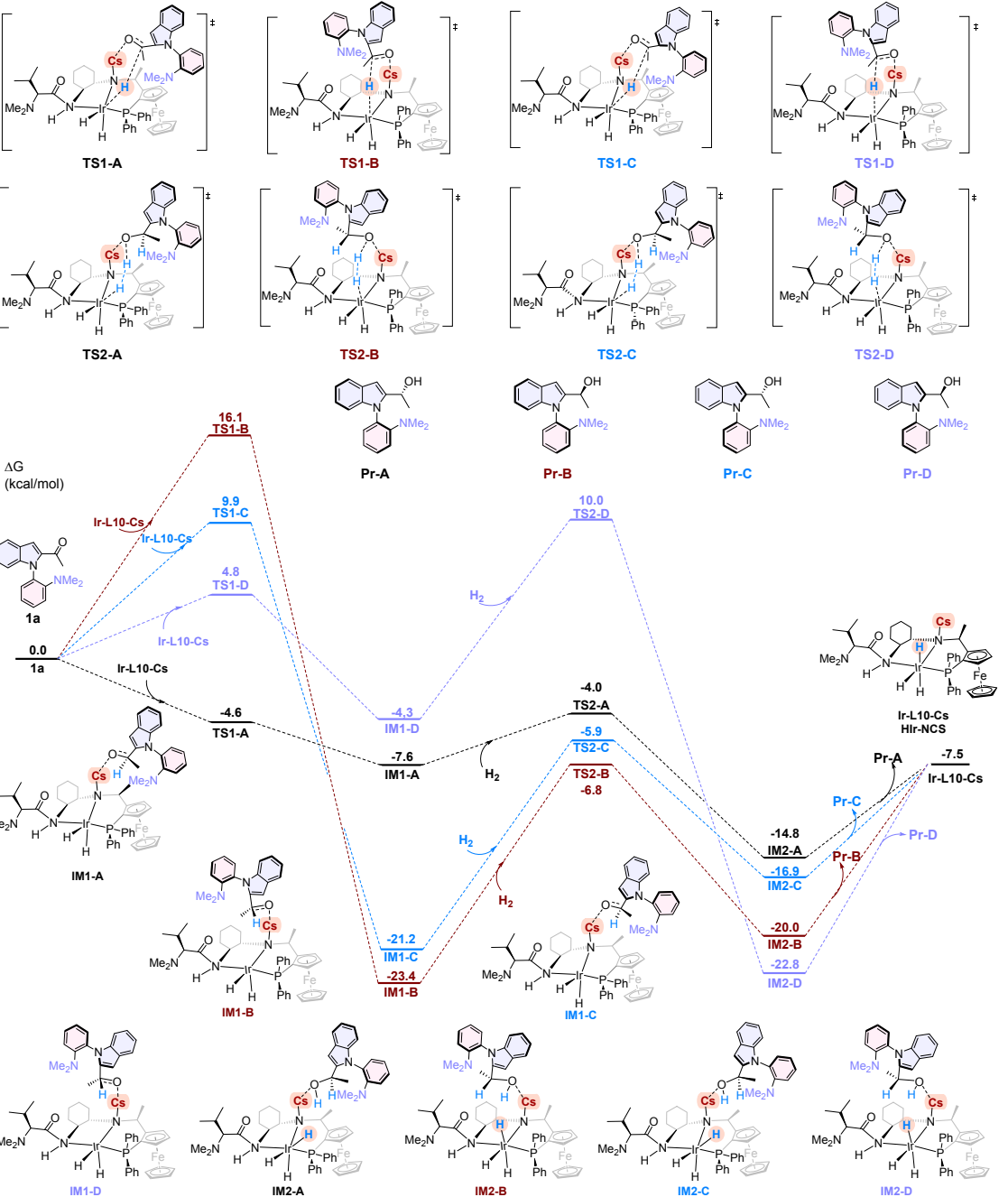


Figure 1. DFT studies on the cesium cation promoted asymmetric hydrogenation process.

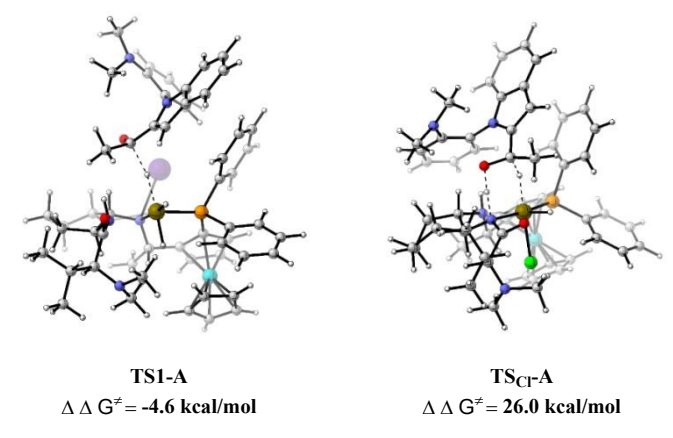


Figure 2. Reaction energy barriers: anionic vs neutral catalytic systems.

the formation of the deprotonated anionic Ir-L10-Cs species as the active catalyst. Moreover, the results from L13 demonstrate that the amino acid moiety plays a significant role in the ligand. The origin of the significant difference in catalytic performance between fdiaphos and Huaphos remains under investigation.

In light of previous literature, [16,17b,17c] we propose that the anionic Ir-L10-Cs (HIr-NCs) and neutral Ir-L10 (HIr-NH) catalysts operate via distinct mechanistic pathways-a hypothesis supported by DFT calculations. For the hydrogenation mechanism of Ir-L10-Cs, as illustrated in Figure 1, the entire process is divided into two stages. In Stage 1, reactant first undergoes hydrogenation at the carbonyl carbon through transition state TS1, a key step that simultaneously establishes both axial chirality and the stereogenic center at the carbonyl carbon, thereby determining the overall stereoselectivity. The relative energy barriers for TS1-A (-4.6 kcal/mol), TS1-B (4.8 kcal/mol), TS1-C (9.9 kcal/mol), and TS1-D (16.1 kcal/mol) govern the preferential formation of Pr-A as the major product. Moreover, the energy differences among these transition states are consistent with the experimental observed enantiomeric excess (>99% ee) and

diastereomeric ratio (>99:1 dr). In Stage 2, molecular hydrogen adds to the IM1 intermediate via TS2, in which one hydrogen atom from H₂ is transferred to the carbonyl oxygen of the substrate, while the other binds to the iridium center. This leads to the formation of IM2, which subsequently releases the final products (Pr-A, Pr-B, Pr-C, and Pr-D) upon catalyst regeneration. To enhance computational efficiency, the simplified model neglects interactions between solvent and cations,[14,17b] as well as the potential effects of carbonate/bicarbonate ions, the latter being particularly challenging to describe accurately with conventional Gaussian-type DFT methods. Importantly, weak π -interactions between toluene and metal ions may occur under actual reaction conditions, potentially modulating conformational equilibria and consequently shifting the activation barriers (Supporting Information for details, page S67-68). A more sophisticated modeling strategy, such as that employed by Poli et al.,[16] would better account for these subtle yet non-negligible factors. In addition, density functional theory (DFT) calculations were performed to investigate the hydrogenation pathway mediated by the neutral Ir-L10 catalyst (Supporting Information, Page S66). In this pathway, hydrogen transfer occurs in a single step via a concerted, bifunctional mechanism: the hydride on iridium attacks the carbonyl carbon, while the amide N-H proton is delivered to the carbonyl oxygen. Although repeated attempts failed to locate a well-defined transition state that fully accounts for the enantioselectivity in the hydrogenation process (Supporting Information for details, Page S65-66), it is noteworthy that the significant energy difference between Ir-L10-Cs and Ir-L10 inherently reflects the substantial advantage of the anionic catalytic system (Figure 2). This difference is primarily attributed to the strong electrostatic interaction between the Cs⁺ cation in Ir-L10-Cs and the carbonyl oxygen of substrate 1a, which stabilizes the transition state and lowers the activation energy. These results indicate that Ir-L10-Cs exhibits substantially enhanced hydrogenation activity compared to Ir-L10, in excellent agreement with experimental observations. Integrated analysis of experimental

Scheme 5. Proposal catalytic cycle for AH under Cs₂CO₃ or CH₃CO₂Li

This article is licensed under a Creative Commons Attribution-NonCommercial 3.0 Unported Licence

Open Access Article. Published on 27 November 2025. Downloaded on 28.11.2025 06:55:37

Scheme 6. Substrate scope of *N*-aryl indole aldehydes

View Article Online DOI: 10.1039/D5SC08462H

Reaction conditions: 8 (0.25 mmol), [Ir(COD)Cl]₂ (0.05 mol%), L9 (0.11 mol%), CH₃CO₂Li (10 mol%), toluene (1 mL), r.t. and H₂ (1.5 MPa). Isolated yields were obtained by flash chromatography and the *ee* value was determined by HPLC analysis.

results, spectroscopic data, and DFT calculations leads to a comprehensive catalytic cycle for the hydrogenation under varying basic conditions (**Scheme 5**). Rapid C-N bond rotation, mediated by a six-membered pericyclic transition state, facilitates dynamic racemization of the substrate. In this framework, the *S*-configured isomer is selectively activated and reduced by either the anionic **Ir-L10-Cs** catalyst or the neutral **Ir-L10** species, leading to product formation.

Strategy Extension. Having successfully accomplished the dynamic kinetic resolution (DKR) of N-aryl indole ketones, we hypothesized that the Ir-catalyzed asymmetric hydrogenation system might also be applicable to N-aryl indole aldehydes. Surprisingly, the optimal ligand for the reaction shifted from **L10** to L9. After brief optimization of the reaction parameters (Supporting Information for details, Page S27-28), the Ir-L9 catalytic system was applied to a series of aldehyde substrates, yielding the corresponding products with moderate to excellent enantioselectivity (Scheme 6). Condition screening revealed a trade-off between reaction rate and stereoselectivity: while Cs₂CO₃ promoted faster conversion, employing CH₃CO₂Li delivered slightly enantioselectivity. On this basis, CH₃CO₂Li was selected as the optimal base for maximizing ee. Consistent with the trend observed for ketones, aldehydes bearing electron-withdrawing groups (9d, 9f-9h, 9k) reacted significantly faster than those with electron-donating substituents (9b, 9c, 9e, 9i, 9j, 9l-9o). In contrast, the latter group

generally afforded higher enantiomeric excess, suggesting that electronic effects influence enantioselectivity differently than reaction kinetics. Unfortunately, compounds **9d** and **9o** showed lower *ee* values, despite their structural similarity to high-performing analogues. This may be attributed to steric hindrance that compromises effective chiral induction during the hydride transfer step. These results highlight the broad substrate scope and excellent stereocontrol achievable with this DKR strategy.

Finally, to elucidate the reaction pathway of N-aryl indole aldehydes, we characterized the catalyst Ir-L9 (see the Supporting Information for details, Page S56-59). The results indicate that its structure is analogous to Ir-L10. Given that the hydrogenation of aldehydes also proceeds under catalysis by CH_3CO_2Li , we propose that the mechanism of Ir-L9-catalyzed aldehyde reduction is analogous to that of Ir-L10-mediated ketone hydrogenation.

Conclusions

In conclusion, we have developed a new class of chiral ferrocene-based tridentate ligands (**Huaphos**) which were used for Ir-catalyzed asymmetric hydrogenation of *N*-aryl indole ketones (and aldehydes) via a dynamic kinetic resolution process under neutral conditions, providing enantiomerically enriched *N*-aryl indole amino alcohols in high yields with excellent stereoselectivity (up to 99% yield, >99% ee, >99:1 dr). Under the influence of Cs_2CO_3 , the **Ir/Huaphos** complex

ARTICLE Journal Name

(HIr-NH) undergoes activation to form an anionic, tridentate iridium catalyst (Ir-L10-Cs), which exhibits significantly enhanced catalytic efficiency. The strong electrostatic interaction between the Cs⁺ cation and the oxygen atom of the substrate effectively lower the reaction barrier, enabling rapid hydrogenation. The reaction can be conducted on a gram scale with a relatively low catalyst loading (S/C = 40,000) in the presence of Ir-L10-Cs (HIr-NCs), and reaction products can be readily transformed into novel chiral ligands, which exhibit promising applications in asymmetric catalysis. Research into the applications of this highly efficient catalyst and related products is still underway.

Author contributions

Xianghua Zhao: conceptualization, data curation, formal analysis, investigation, methodology, validation, visualization, writing — original draft, writing — review & editing; Xinyu Chen, Linxian Fan and Yulong Jiang: investigation and data curation. Yirui Chen and Dinguo Song: Project administration. Junyuan Hu: resources, software (DFT calculations), visualization; Fei Ling and Weihui Zhong: funding acquisition, project administration, resources, supervision.

Conflicts of interest

There are no conflicts to declare.

Data availability

All experimental procedures and data related to this study can be found in the ESI. \dagger

Acknowledgements

We thank the financial supports from the National Natural Science Foundation of China (Nos. 22378363, 22178315 and 22578417), Natural Science Foundation of Zhejiang Province (No. LQ24B060008) and Key Research and Development Program of Zhejiang Province (No. 2023C03117). And we sincerely thank Ms. Minna Zhi, a graduate of the School of Chemistry and Molecular Engineering at Nanjing Tech University, for her meticulous and patient assistance with the DFT calculations.

Notes and references

- S. E. Clapha. m, A. Hadzovic, R. H. Morris, Coord. Chem. Rev. 2004, 248, 2201-2237.
- a) T. Ohkuma, H. Ooka, S. Hashiguchi, T. Ikariya, R. Noyori, J. Am. Chem. Soc. 1995, 117, 2675–2676. b) S. Hashiguchi, R. Noyori, Acc. Chem. Res. 1997, 30, 97–102. c) T. Ohkuma, M. Koi-zumi, H. Doucet, T. Pham, M. Kozawa, K. Murata, E. Katayama, T. Yokozawa, T. Ikariya, R. Noyori, J. Am. Chem. Soc. 1998, 120, 13529–13530. d) R. Noyori, T. Ohkuma, Angew. Chem. Int. Ed. 2001, 40, 40-73.
- 3. a) K. J. Haack, S. Hashiguchi, A. Fujii, T. Ikariya, R. Noyori, *Angew. Chem. Int. Ed.* **1997**, *36*, 285-288. b) M. Yamakawa, H. Ito, R.

- Noyori, *J. Am. Chem. Soc.* **2000**, *122*, 1466–1478. c) K. A. Rashid. S. E. Clapham, A. Hadzovic, J. N. Harvey, P.J. Lough/R5AC Morals, *J. Am. Chem. Soc.* **2002**, *24*, 15104–15118. d) R. Sandoval, T. Ohkuma, K. Muniz, R. Noyori, *J. Am. Chem. Soc.* **2003**, *125*, 13490-13503. e) C. A. Sandoval, Y. Yamaguchi, T. Ohkuma, K. Kato, R. Noyori, *Magn. Reson. Chem*, **2006**, *44*, 66-75. f) P. A. Dub, J. C. Gorden, *Nat. Rev. Chem.* **2018**, *2*, 396-408.
- a) J. H. Xie, X. Y. Liu, J. B. Xie, L. X. Wang, Q. L. Zhou, Angew. Chem. Int. Ed. 2011, 50, 7329-7332. b) D. H. Bao, H. L. Wu, C. L. Liu, J. H. Xie, Q. L. Zhou, Angew. Chem. Int. Ed. 2015, 54, 8791-8794. c) F. H. Zhang, C. Wang, J. H. Xie, Q. L. Zhou, Adv. Synth. Catal. 2019, 361, 2832-2835. d) F.-H. Zhang, F.-J. Zhang, M.-L. Li, J.-H. Xie, Q.-L. Zhou, Nat. Catal. 2020, 3, 621-627.
- a) W. Wu, S. Liu, M. Duan, X. Tan, C. Chen, Y. Xie, Y. Lan, X. Dong, X. Zhang, Org. Lett. 2016, 18, 2938-2941. b) L. Zeng, H. Yang, M. Zhao, J. Wen, J. H. R. Tucker, X. Zhang, ACS Catal. 2020, 10, 13794-13799. c) J. Yu, F. Huang, W. Fang, C. Yin, C. Shi, Q. Lang, G.-Q. Chen, X. Zhang, Green Synth. Catal. 2022, 3, 175-178.
- a) A. A. Mikhailine, M. I. Maishan, A. J. Lough, R. H. Morris, *J. Am. Chem. Soc.* 2012, *134*, 12266-12280. b) W. Zuo, A. J. Lough, Y. Li, R. H. Morris, *Science* 2013, *342*,1080-1083. c) P. O. Lagaditis, P. E. Sues, J. F. Sonnenberg, K. Y. A. J. Wan, Lough, R. H. Morris, *J. Am. Chem. Soc.* 2014, *136*, 1367-1380.
- M. B. Widegren, G. J. Harkness, A. M. Z. Slawin, D. B. Cordes, M. L. Clarke, *Angew. Chem. Int. Ed.* 2017, *56*, 5825-5828.
- a) M. Garbe, Z. H. Wei, B. Tannert, A. Spannenberg, H. J. Jiao, S. Bacumann, M. Scalone, K. Junge, M. Beller, *Adv. Synth. Catal.* 2019, 361, 1913-1920. b) M. Garbe, K. Junge, S. Walker, Z. H. Wei, H. J. Jiao, A. Spannenberg, S. Bacumann, M. Beller, *Angew. Chem. Int. Ed.* 2017, 56, 11237-11241.
- a) N. Abbas, Y. B. Wan, X.-P. Hu, J. Org. Chem. 2025, 90, 9667-9671. b) Y. Y. Li, K. Lu, J. S. Yang, X. M. Zhang, F. M. Zhang, Y. Q. Tu, Nat. Commun. 2025, 16, 6078. c) J. Yang, Y. Guo, Z. Wang, Y. Fu, D. Wang, Q. Liu, G. A. Solan, Y. Ma, W. H. Sun, Org. Lett. 2025, 27, 2564-2568. d) S. Paira, N. Jain, D. Adhikari, R. B. Sunoj, B. Sundararaju, Chem. Sci. 2025, 16, 13826-13837. e) Z. M. Wang, M. H. Li, W. W. Zuo, J. Am. Chem. Soc. 2024, 146, 26416-26426.
- E. S. Wiedner, M. B. Chambers, C. L. Pitman, R. M. Bullock, A. J. M. Miller, A. M. Appel, *Chem. Rev.* **2016**, *116*, 8655-8692.
- a) R. A. Grey, G. P. Pez, A. Wallo, J. Am. Chem. Soc. 1980, 102, 5948-5949.
 b) R. A. Grey, G. P. Pez, A. Wallo, J. Corsi, J. Chem. Soc. Chem. Commun. 1980, 16, 783-784.
 c) G. P. Pez, R. A. Grey, J. Corsi, J. Am. Chem. Soc. 1981, 103, 7528-7535.
 d) R. A. Grey, G. P. Pez, A. Wallo, J. Am. Chem. Soc. 1981, 103, 7536-7542.
 e) R. A. Grey, G. P. Pez, A. Wallo, J. Corsi, Ann. New York Acad. Sci. 1983, 415, 235-243.
- a) M. Nielsen, E. Alberico, W. Baumann, H-J. Drexler, H. Junge, S. Gladiali, M. Beller, *Nature*, 2013, 495, 85–89. b) E. Alberico, A. J. J. Lennox, L. K. Vogt, H. Jiao, W. Baumann, H-J. Drexler, M. Nielsen, A. Spannenberg, M. P. Checinski, H. Junge, M. Beller, *J. Am. Chem. Soc.* 2016, 138, 14890-14904. c) C. Liu, R. V. Putten, P. O. Kulyaev, G. A. Filonenko, E. A. Pidko, *J. Catal.* 2018, 363, 136–143.
- a) R. Hartmann, P. Chen, Angew. Chem. Int. Ed. 2001, 40, 3581-3585.
 b) R. Hartmann, P. Chen, Adv. Synth. Catal. 2003, 345, 1353-1359.

This article is licensed under a Creative Commons Attribution-NonCommercial 3.0 Unported Licence

Den Access Article. Published on 27 November 2025. Downloaded on 28.11.2025 06:55:37

ARTICLE Journal Name

- 14. P. A. Dub, N. J. Henson, R. L. Martin, J. C. Gordon, J. Am. Chem. Soc. 2014, 136, 3505-3512.
- 15. a) J. M. John, S. Takebayashi, N. Dabral, M. Miskolzie, S. H. Bergens, J. Am. Chem. Soc. 2013, 135, 8578-8584. b) S. Nakane, T. Yamamura, S. K. Manna, S. Tanaka, M. Kitamura, ACS Catal. **2018**, *8*, 11059-11075.
- 16. a) J. M. Hayes, E. Deydier, G. Ujaque, A. Lledos, R. M. Kabbara, E. Manoury, S. Vincendeau, R. Poli, ACS Catal. 2015, 5, 4368-4376. b) P. Kisten, S. Vincendeau, E. Manoury, J. M. Lynam, J. M. Slattery, S. B. Duckett, A. Lledos, R. Poli, Chem. Sci. 2024, 15, 20478-20492.
- 17. a) Y. Wang, S. Liu, H. Yang, H. Li, Y. Lan, Q. Liu, Nat. Chem. 2022, 14, 1233-1241. b) C. Yin, F. Jiang, Y. F. Huang, C. Q. Xu, Y. Pan, S. Gao, G. Q. Chen, X. Ding, S. T. Bai, Q. Lang, J. Li, X. Zhang, Nat. Commun. 2023, 14, 3718. c) M. Wang, S. Liu, H. Liu, Y. Wang, Y. Lan, Q. Liu, Nature 2024, 631, 556-562.
- 18. a) K. P. Manfredi, J. W. Blunt, J. H. Cardellina, J. Med. Chem. 1991, 34, 3402-3405. b) M. R. Boyd, Y. F. Hallock, K. P. Manfredi, J. Med. Chem. 1994, 37, 1740-1745. c) G. Bringmann, T. Gulder, T. A. M. Gulder, Chem. Rev. 2011, 111, 563-639. d) L. Pu, Chem. Rev. 2004, 104, 1687-1716. e) G. Dotsevi, Y. Sogah, D. J. Cram, J. Am. Chem. Soc. 1976, 98, 3038-3041. f) Q. Li, L. Green, N. Venkataraman, J. Am. Chem. Soc. 2007, 129, 12908- 12909. g) M. Berthod, G. Mignani, G. Woodward, Chem. Rev. 2005, 105, 1801-1836. h) M. Shibasaki, S. Matsunaga, Chem. Soc. Rev. 2006, 35, 269-279. i) B. V. Rokade, P. J. Guiry, ACS Catal. 2018, 8, 624-643.
- 19. a) S. J. Liu, X. Wang, J. X. Yang, X. S. Ao, S. F. Ni, Y. C. Zhang, F. Shi, Nat. Commun. 2025, 16, 6605. b) H. H. Zhang, T. Z. Li, S. J. Liu, F. Shi, Angew. Chem. Int. Ed. 2024, 63, e202311053. c) H. Liu, Z. Qi, Y. Shi, W. Wang, F. Wang, Z. W. Ding, A. Q. Jia, G. Huang, X. Li, Nat. Commun. 2025, 16, 5741. d) Janabel, D. Kumar, V. V. Kanale, M. Liu, C. Uyeda, J. Am. Chem. Soc. 2025, 147, 23270-23276. e) . Q. Bian, L. Qin, L. W. Fan, J. Fu, Y. F. Cheng, Y. F. Zhang, Q. Song, P. F. Wang, Z. L. Li, Q. S. Gu, P. Yu, J. B. Tang, X. Y. Liu, Nat. Commun. 2025, 16, 4922. f) J. M. Coto-Cid, G. de A. Carmona, J. Iglesias-Sigüenza, Gonzalo. J. Rodríguez-Salamanca, R. Fernández, V. Hornillos, J. M. Lassaletta, Adv. Synth. Catal. 2024, 366, 909-915. g) X. Hao, Z. Tian, Z. Yao, T. Zang, S. Song, L. Lin, T. Qiao, L. Huang, H. Fu,

- Angew. Chem. Int. Ed. 2024, 63, e202410112. h) Dai Y. Liu, Q. Xu, M. Wang, Q. Zhu, P. Yu, G. Zhong, XO Zeng, Angew. Chen. Int. Ed. 2023, 62, e202216534. i) Y.-D. Shao, D.-D. Han, H.-X. Jiang, X.-Y. Zhou, W.-K. Wang, J.-X. Zhang, Y.-F. Liu, D.-J. Cheng, Org. Chem. Front. 2024, 11, 3894-3899. j) P. Rodríguez-Salamanca, G. de Gonzalo, J. A. Carmona, J. López-Serrano, J. Iglesias-Sigüenza, R. Fernández, J. M. Lassaletta, V. Hornillos. ACS Catal. 2022, 13, 659-664. K) D. Y. Wang, J. Y. Zong, B. W. Wang, L. W. Sun, X. Xiao, H. R. Piao, F. E. Chen, Green Synth. Catal. 2025, 6, 211-215.
- 20. a) G. Q. Chen, B. J. Lin, J. M. Huang, L. Y. Zhao, Q. S. Chen, S. P. Jia, Q. Yin, X. Zhang, J. Am. Chem. Soc. 2018, 140, 8064-8068. b) Y.-B. Wan, X.-P. Hu, ACS Catal. 2022, 14, 17633-17641. c) T. Niu, L.-X. Liu, Y.-Q. Bai, H.-W. Li, B. Wu, Y.-G. Zhou, Sci. China Chem. **2025**, 68, 4984-4990.
- 21. a) F. Ling, S. Nian, J. Chen, W. Luo, Z. Wang, Y. Lv, W. Zhong, J. Org. Chem. 2018, 83, 10749-10761. b) F. Ling, H. Hou, J. Chen, S. Nian, X. Yi, Z. Wang, D. Song, W. Zhong, Org. Lett. 2019, 21, 3937-3941. c) X. Yi, Y. Chen, A. Huang, D. Song, J. He, F. Ling, W. Zhong, Org. Chem. Front. 2021, 8, 6830-6836. d) Z. Wang, X. Zhao, A. Huang, Z. Yang, Y. Cheng, J. Chen, F. Ling, W. Zhong, Tetrahedron Lett. 2021, 82.
- 22. V. Hornillos, J. A. Carmona, A. Ros, J. Iglesias-Siguenza, J. Lopez-Serrano, R. Fernandez, J. M. Lassaletta, Angew. Chem. Int. Ed. **2018**, *57*, 3777-3781.
- 23. a) X. Hong, J. Guo, J. Liu, W. Cao, C. Wei, Y. Zhang, X. Zhang, Z. Fu, Sci. China Chem. 2022, 65, 905-911.b) Y. Chen, Y. Cheng, W. Tong, H. Wu, C. Zhao, D. Song, F. Ling, W. Zhong, Green Chem. 2025, 27, 7717-7727. c) M. Zhang, T. Niu, M. Liang, F. Xu, Y. Du, H. Zhuang, R. J. Song, H. Yang, Q. Yin, J. Am. Chem. Soc. 2025, 147, 18197-18207. d) M. Liao, J. Li, H. Zhu, Z. Han, Y. Zhang, J. Sun, H. Huang, Org. Lett. 2025, 27, 4836-4841.
- 24. a) X. Han, F. Zhong, Y. Wang, Y. Lu, Angew. Chem. Int. Ed. 2012, 51, 767-70. b) X. Xiao, B. Shao, J. Li, Z. Yang, Y. J. Lu, F. Ling, W. Zhong, Chem. Commun. 2021, 57, 4690-4693. c) N. Abbas, Y. B. Wan, X. P. Hu, J. Org. Chem. 2025, 90, 9667-9671. d) J. Yang, Y. Guo, Z. Wang, Y. Wang, D. Fu, Q. Liu, G. A. Solan, Y. Ma, W. H. Sun, Org. Lett. 2025, 27, 2564-2568. e) L. Z. Zhang, P. C. Zhang, Q. Wang, M. Zhou, J. Zhang, Nat. Commun. 2025, 16, 930.

Data Availability Statement

Title: Bulky Alkali Metal Cations Enabled Highly Efficient Iridium-Catalyzed Asymmetric Hydrogenation for C–N Axial Chirality via Dynamic Kinetic Resolution

Author: Xianghua Zhao, Xinyu Chen, Linxian Fan, Yulong Jiang, Yirui Chen, Dingguo Song, Fei Ling*, Junyuan Hu* and Weihui Zhong*

Data availability

This article is licensed under a Creative Commons Attribution-NonCommercial 3.0 Unported Licence.

Open Access Article. Published on 27 November 2025. Downloaded on 28.11.2025 06:55:37.

All experimental procedures and data related to this study can be found in the ESI. \dagger